Radiation Protection Dosimetry (2007), Vol. 126, No. 1–4, pp. 278–283 doi:10.1093/rpd/ncm058
Advance Access publication 23 May 2007

NOVEL Al_2O_3:C,Mg FLUORESCENT NUCLEAR TRACK DETECTORS FOR PASSIVE NEUTRON DOSIMETRY

G. Jeff Sykora[1], Mark S. Akselrod[1,*], M. Salasky[2] and Stephen A. Marino[3]
[1]Landauer, Inc., Stillwater Crystal Growth Division, 723 $\frac{1}{2}$ Eastgate, Stillwater, OK 74074, USA
[2]Landauer Inc., 2 Science Rd., Glenwood, IL 60425, USA
[3]RARAF Columbia University, 136 S. Broadway, Irvington, NY 10533, USA

The latest advances in the development of a fluorescent nuclear track detector (FNTD) for neutron and heavy charged particle dosimetry are described and compared with CR-39 plastic nuclear etched track detectors (PNTDs). The technique combines a new luminescent aluminium oxide single crystal detector (Al_2O_3:C,Mg) with an imaging technique based on laser scanning and confocal fluorescence detection. Detection efficiency was obtained after irradiations with monoenergetic neutron and proton beams. Dose dependences were measured for different configurations of the detectors exposed in fast- and thermal-neutron fields. A specially developed image processing technique allows for fast fluorescent track identification and counting. The readout method is non-destructive, and detectors can be reused after thermal annealing.

INTRODUCTION

Passive nuclear track detectors are attractive for neutron dosimetry because they have 100% n/γ discrimination. For instance, CR-39 plastic nuclear track detectors (PNTD)[(1)] have high sensitivity, but are not reusable, require long processing time and extensive chemical etching. Recently, Landauer developed a novel passive fluorescent nuclear track detector (FNTD) based on single aluminium oxide crystals doped with carbon and magnesium and having aggregate oxygen vacancy defects (Al_2O_3:C,Mg)[(2–4)]. The newly developed FNTDs are more in common with CR-39 PNTDs, in that individual particle tracks can be imaged and counted and particle trajectories can be traced through the volume of the detector. This new FNTD technology is capable of optical and non-destructive detection of charged particles with linear energy transfer (LET) in water as low as 0.5 keV μm^{-1} while maintaining the ability to measure charged particles with higher LET. Diffraction-limited optical resolution of the method allows detection of high doses and fluences up to $10^7 cm^{-2}$ without saturation. The detectors can be completely erased using thermal annealing and reused. In comparison with optically stimulated luminescent detectors (OSLD), the new detectors use very deep traps and thus are very thermally and optically stable and do not require protection from visible light.

Presented at the 10th International Symposium on Neutron Dosimetry, Uppsala, Sweden 12–16th June 2006, Paper B1-14.
*Corresponding author: makselrod@landauerinc.com

MATERIALS AND METHODS

The FNTD is made of aluminium oxide single crystal doped with carbon and magnesium (Al_2O_3:C,Mg). 'As-grown' or annealed crystals contain high concentrations of aggregate F_2^{2+} (2Mg)-colour centres that are believed to consist of two oxygen vacancies charge compensated by two Mg ions. Details of spectroscopic properties of the new crystals can be found elsewhere[(5)]. Laser-induced fluorescence in this crystal can be stimulated with a 635-nm red laser diode without photoionisation of the colour centres, thus allowing non-destructive readout. Luminescence decay time of the new colour centre is almost 1 million times faster than that of the F-centre in Al_2O_3:C OSL material, making it possible to perform fast and non-destructive imaging of the crystal.

For this study, 50 samples were cut from Al_2O_3:C,Mg crystals along the optical axis into small rectangular plates ($6 \times 10 \times 1\ mm^3$) and polished on their large sides.

Irradiations with monoenergetic neutrons and protons were performed at the Radiological Research Accelerator Facility (RARAF) of Columbia University. Twenty-seven bare detectors without any converter on them were exposed to protons to a fluence of around $2 \times 10^4\ mm^{-2}$ with energies of 0.3, 0.59, 1.5 and 2.9 MeV. Most of the proton irradiations were performed at normal angle of incidence to the detector surface, and several samples were irradiated with 1.5-MeV protons at 30°, 60° and 90°. Sixteen detectors were also irradiated at RARAF with monoenergetic neutrons. Neutrons with energy of 0.2, 0.5, 1.0 and 2.0 MeV were produced through T(p,n)^{3}He reaction, 6-MeV neutrons were produced by D(d,n)^{3}He reaction and 14-MeV

neutrons were generated by T(d,n)^{4}He reaction using a Van de Graff proton accelerator. All detectors for neutron irradiations had only two converters: 1 mm polyethylene (PE) and 1 mm ^{10}B-loaded Teflon (10% by weight) having area of 10 by 10 mm^2, placed directly on top of them.

Dose dependences were obtained after irradiation with fast and thermal neutrons from calibrated Am–Be neutron sources at the Landauer irradiation facility. Delivered $H_p^*(10)$ doses were in the range from 0.3 to 300 mSv for fast neutrons and from 0.3 to 10 mSv for thermal neutrons. Irradiations with fast neutrons were performed using a 185 MBq Am–Be source in two geometries: 'free-in-air' at 20 cm from the source and on a $30 \times 30 \times 15$-cm^3 PMMA phantom at 50 cm distance. Thermal neutrons were produced by a 37-MBq Am–Be source moderated by 180 mm of paraffin. All detectors exposed in this experiment to both fast and thermal neutrons had the same configuration with three areas covered by 1 mm of PE converter, 1 mm of ^{10}B-loaded Teflon and a ^{6}LiF TLD-600 chip having 4.5 mm in diameter.

Optical imaging of the detectors was performed using a new experimental set-up custom-built at Stillwater R&D laboratories of Landauer. The system is based on a classical scheme of the laser scanning fluorescence confocal microscope and is described elsewhere[2].

The detector is first scanned perpendicular to the detector surface using a piezoelectric actuator to detect the surface position with an accuracy of 0.1 μm and then imaged at the desired depth—usually at 1 μm below the surface. An example of the image obtained after fast-neutron irradiation is presented in Figure 1. Multiple images were obtained from FNTD behind each of the three converters. The imaged area has dimensions of 150×150 μm^2. The number of acquired images depends on the density of tracks and adaptively varies between 1 and 25 for each of the three converter areas. The images are processed and tracks are identified and counted either by an automatic track processing program synchronously with scanning of the next image or manually from the saved file to ensure the quality of automatic processing.

Confocal fluorescence microscopy allows for stimulation of a highly localised volume of the crystal and diffraction-limited spatial resolution. Because of radiochromic transformations the intensity of fluorescence induced within the track volume is stronger than that induced outside the track.

The materials and methods used for the CR-39 etched track detectors from Landauer tested in this study are similar to that described in detailed elsewhere[1].

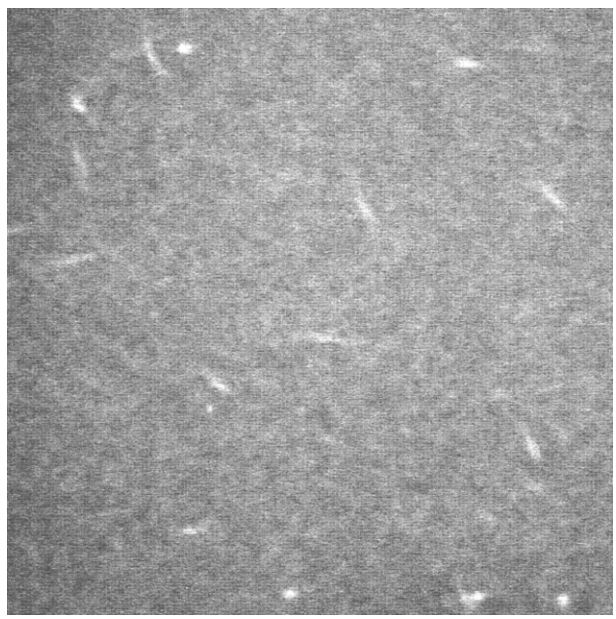

Figure 1. Image of recoil proton tracks obtained from Al_2O_3:C,Mg FNTD in fluorescent contrast using confocal laser scanning system. The tracks were produced behind the PE converter using fast neutron irradiation from Am–Be source. Image size is 100×100 μm^2.

RESULTS

Proton irradiations

The dose of fast neutrons is measured in FNTD technology through detection of recoil protons generated by neutrons in a PE converter. Thus, investigation of the FNTD detection efficiency and fluorescence track amplitude as a function of proton energy and angle of incidence is critically important. The range of protons in Al_2O_3 was also compared with that calculated using SRIM-2003 software[6].

Comparison of delivered fluences that were calculated from the accelerator instrumentation data and the measured FNTD track density yields the detector efficiency that is practically 100% for protons within the investigated energy range. Discrepancies between delivered and measured fluences are between 0.3 and 8% for different samples and might be caused by the errors in irradiation time and beam instrumentation coupled with statistical fluctuations of the requested low fluences.

Fluorescence amplitudes of tracks induced by monoenergetic protons were investigated as a function of proton energy. A special automatic image processing routine was developed in LabView to process a large number of tracks for each sample. Figure 2 shows the dependence of amplitude on proton energy. Histograms of track amplitude distributions are shown on the insert. The spread in amplitudes is probably due to two main factors: an uneven distribution of colour centres within the detector and the spread in proton energies. As the LET_∞ of the protons decreases with increasing energy, the amplitudes of the tracks start to reach saturation. In the same experiment CR-39 detectors were exposed. As one can see from Figure 2, the pit diameter of proton tracks decreases exponentially with the energy and does not change much for energies above 2 MeV. For FNTD, the measured fluorescent track diameter does not change with the proton energy because the track core is very small (on the order of a few nanometers) compared with the spot size of the excitation beam ($\sim\lambda/NA$). All tracks appear to be $\sim$1 μm in diameter for protons penetrating perpendicular to the detector surface and $\sim$1 μm in width for the angled tracks.

The length of the imaged track increases linearly with the angle of incidence making it easy to determine the angle. The confocal geometry of the optical readout system allows the detector to be imaged at multiple depths and provides information about the particle range[3]. In this study, 3-D images of 1.5-MeV proton tracks penetrating the detector were also acquired and a range of 16.0 ± 0.5 μm was determined. Calculation using SRIM-2003[6] gave us 16.49 μm, in good agreement with the measured value.

Detector responses to monoenergetic neutrons

The neutron detection efficiency as a function of neutron energy for both CR-39 and FNTD is shown in Figure 3. Two competing processes affect the efficiency of FNTD. At low energies, a limiting factor is a small recoil proton range, whereas at higher neutron energies (n,p), scattering cross section decreases as $1/\sqrt{E}$. The maximum recoil proton energy from a PE converter for a 0.2-MeV neutron irradiation is 0.2 MeV, and the maximum proton range in Al_2O_3 as calculated by SRIM 2003[6] is only 1.08 μm. Short range of low energy recoil protons makes it difficult to detect tracks using fluorescence technique.

In the case of FNTD, the detection efficiency in tracks per incident neutron increases to a maximum value at $\sim$6 MeV (Figure 3), in correspondence with the earlier CR-39 measurements of Benton *et al.*[1].

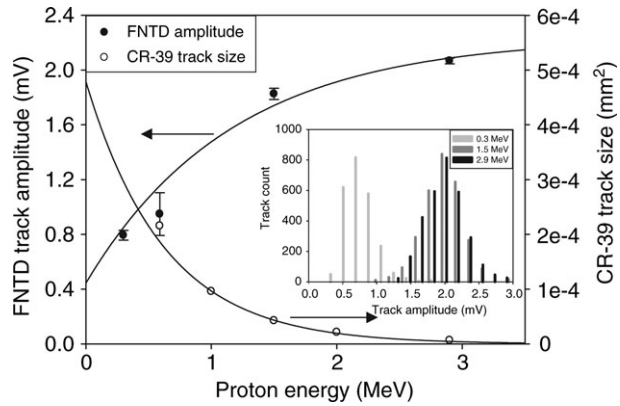

Figure 2. Comparison of track parameters for CR-39 plastic nuclear track detector (track diameter) and Al_2O_3:C,Mg FNTD (fluorescence amplitude) and histogram of distribution of fluorescent amplitudes for three proton energies.

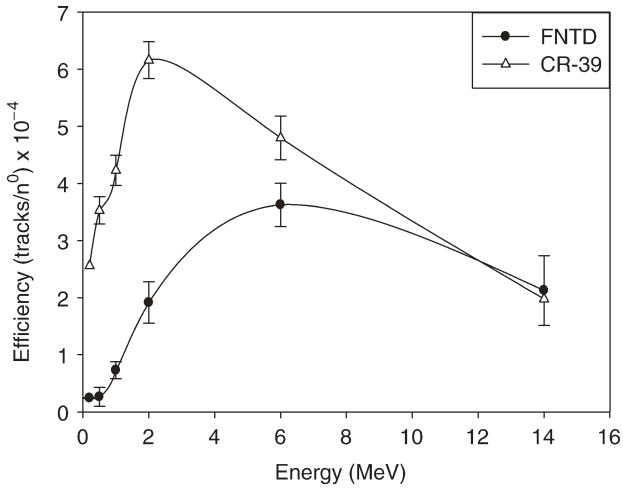

Figure 3. Detection efficiency as a function of energy for monoenergetic neutrons for CR-39 PNTD and Al_2O_3:C,Mg FNTD.

CR-39 detectors from Landauer tested in this study show a peak detection efficiency at 2 MeV with rapid decrease in efficiency at higher energy. An earlier version of Al_2O_3:C,Mg crystals with detection efficiency lower than CR-39 was used in this test. The FNTDs used later for the dose dependencies described below show almost three times higher detection sensitivity, as was confirmed by additional tests performed after 0.2- and 0.5-MeV neutron irradiations at RARAF.

Neutron dose dependence

Multiple images were automatically acquired from each detector from the areas behind all three converters. Dose dependences are presented in Figure 4 and show good linearity within three orders of investigated dose range for fast neutrons. There is no significant difference in the sensitivity of FNTD behind the PE converters between irradiations performed in-air and on-phantom (Figure 4a), which indicates that albedo neutrons do not affect the sensitivity of the detectors to fast neutrons.

The obtained sensitivity of 21.5 tracks mm^{-2} mSv^{-1} is consistent with our preliminary results[2]. In comparison, the sensitivity of CR-39 to fast neutrons is 12.1 tracks mm^{-2} mSv^{-1}. The sensitivity of FNTDs to thermal neutrons with ^{6}LiF converter as determined from the slope of the dose dependence in Figure 4d is 6500 tracks mm^{-2} mSv^{-1}, which is also consistent with the sensitivity reported previously. The track density per 1 mSv of dose for a thermal component of FNTD obtained using ^{6}LiF is 300 times higher than for a PE component which makes it almost insensitive to fast neutrons. As a result, it was concluded that the PE component of the detector is sensitive only to fast neutrons and the ^{6}LiF part provides response exclusively to a thermal component of the field. ^{10}B-loaded Teflon converter gave us almost 100 times lower track density (Figure 4d).

Significant numbers of tracks measured behind the PE converters after irradiations with the paraffin-moderated Am–Be source (Figure 4d) prove that there is still a large flux of fast neutrons in the field. Using the fast neutron sensitivity of 21.5 mm^{-2} mSv^{-1} obtained above from Figure 4a, it was calculated that the dose equivalent of fast neutrons in the 'thermal field' exceeds five times the dose equivalent for thermal neutrons. In turn, detectors behind ^{6}LiF and ^{10}B converters allowed us to estimate the contribution of thermal dose during irradiations with fast neutrons free-in-air and on-phantom due to scattering and albedo neutrons (Figure 4b and c). Using the sensitivity to thermal neutrons of 6500 mm^{-2} mSv^{-1}, it was calculated that the contribution of thermal neutrons during 'free-in-air' irradiations is only 0.1%, whereas during 'on-phantom' irradiations their contribution increased almost 10 times. Scattering of fast neutrons from the concrete walls (3–4 m distance) and the ceiling (1.5 m distance) should contribute at least 5% of the total dose. Most of these scattered neutrons are epithermal and are not detected by FNTD in the current configuration.

Another important observation is the difference in track density for ^{6}LiF and ^{10}B converters obtained after irradiations in different neutron fields

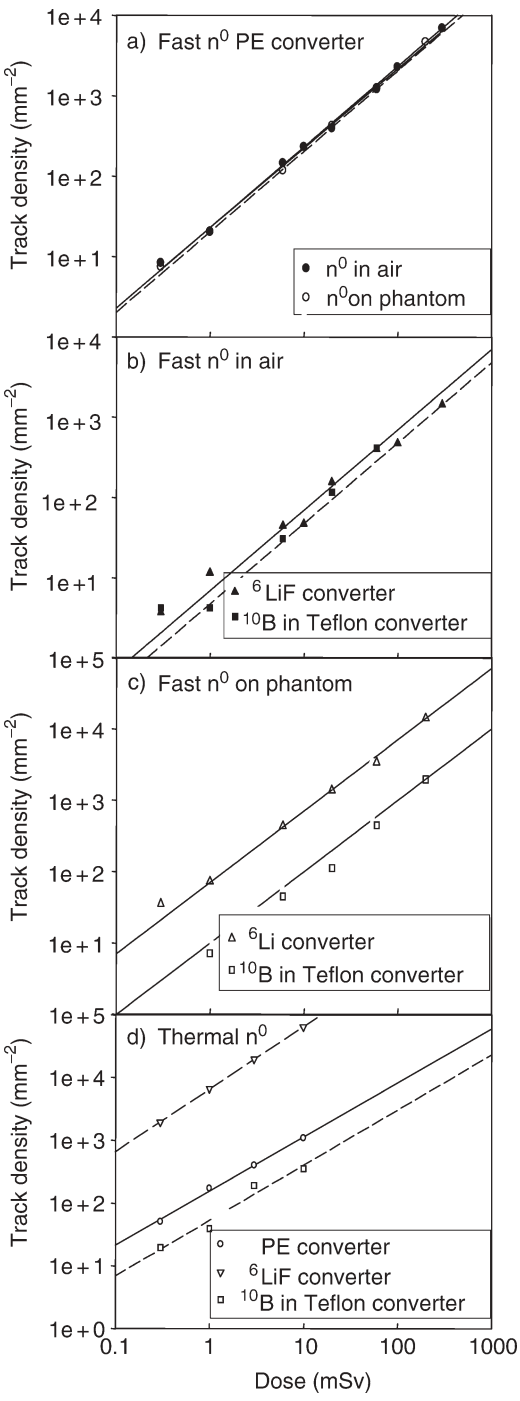

Figure 4. Dose dependences of track densities for Al_2O_3:C,Mg FNTDs covered by three different converters (polyethylene, ^{6}LiF chip and ^{10}B-loaded Teflon) and irradiated with unmoderated and moderated paraffin Am–Be sources.

(see Figure 4b–d). For neutrons moderated by paraffin with a large thermal component, a ^{6}Li converter provides significantly higher response than the ^{10}B converter (Figure 4d), whereas for 'free-in-air' fast neutron irradiations their sensitivity is almost equal (Figure 4b). The albedo configuration during 'on-phantom' irradiations shows the intermediate situation (Figure 4c).

The nuclear reaction and product energies for ^{6}Li(n,α) and ^{10}B(n,α) are as follows:

$$^6\mathrm{Li} + {}^1\mathrm{n} \rightarrow {}^4\mathrm{He}(2.05\,\mathrm{MeV}) + {}^3\mathrm{H}(2.73\,\mathrm{MeV})$$

$$^{10}\mathrm{B} + {}^1\mathrm{n} \rightarrow {}^7\mathrm{Li}^*(0.84\,\mathrm{MeV}) + {}^4\mathrm{He}(1.47\,\mathrm{MeV}) \quad (1)$$

The thermal neutron capture cross section for ^{10}B is about four times that for ^{6}Li, but the Q value of the ^{6}Li(n,α) reaction is about twice that of the ^{10}B(n,α) reaction.

Because both products of the ^{6}Li(n,α) reaction have higher energies, their range is longer and thus easier to detect using FNTD than the products from the ^{10}B(n,α) reaction. The tritium ion has a range of ~24 μm in Al_2O_3 whereas the alpha particle has a range of ~4 μm, as calculated by SRIM 2003[6]. In turn, the range of alpha particles produced in the ^{10}B(n,α) reaction is only 2.9 μm and explains a low detection efficiency of this converter. It has been concluded that an element with high ^{6}Li content is a better choice for a converter of thermal neutrons to be used with FNTD.

CONCLUSIONS

New fluorescent nuclear track detectors based on Al_2O_3:C,Mg single crystals were tested and calibrated in parallel with CR-39 PNTD in different neutron fields and with monoenergetic protons. Good fast to thermal neutron discrimination was demonstrated. The sensitivity and efficiency for these two types of neutron detectors was shown to be comparable while continuing to exhibit 100% n/γ discrimination. At the same time, FNTDs do not require long chemical etching, can measure significantly higher neutron dose and proton fluence due to small track size and are completely reusable and allow for fast automated image processing.

AKNOWLEDGEMENTS

The work of S.A.M. at RARAF of Columbia University was partially supported by Department of Energy (DOE) grant #DE-FG02-01ER63226 and by National Institute of Biomedical Imaging and Bioengineering (NIBIB) grant #8P41EB002033-011). We also want to thank our colleagues at

Landauer: T. H. Underwood, K. Dillin and J. Allen for their contributions to the development of crystal growth technology and sample preparation.

REFERENCES

1. Benton, E. V., Oswald, R. A., Frank, A. L. and Wheeler, R. V. *Proton recoil neutron dosimeter for personnel monitoring*. Health Phys. **40**, 801–809 (1981).
2. Akselrod, M. S., Yoder, R. C. and Akselrod, G. M. *Confocal Fluorescent Imaging of Tracks from Heavy Charged Particles Utilizing New Al_2O_3:C,Mg crystals*. Rad. Prot. Dosim. **119**, 357–362 (2006).
3. Akselrod, G. M., Akselrod, M. S., Benton, E. R. and Yasuda, N. *A Novel Al_2O_3 Fluorescent Nuclear Track Detector for Heavy Charged Particles and Neutrons*. Nucl. Instr. Methods. **B247**, 296–306 (2006).
4. Akselrod, M. S. and Akselrod, A. E. New Al_2O_3:C,Mg crystals for radiophotoluminescent dosimetry and optical imaging of tracks produced by heavy charge particles, Radiat Prot. Dosim. **119**, 218–221 (2006).
5. Akselrod, M. S., Akselrod, A. E., Orlov, S. S., Sanyal, S. and Underwood, T. H. *Fluorescent aluminum oxide crystals for volumetric optical data storage and imaging application*. J. Fluoresc., **13**, 503–511 (2003).
6. Ziegler, J. F. and Biersack, J. P. *SRIM-2003.20 software package*. Available on http://www.srim.org/.